Detection of Lung Nodule Candidates in Chest Radiographs

Carlos S. Pereira[1,2], Hugo Fernandes[1], Ana Maria Mendonça[1,2], and Aurélio Campilho[1,2]

[1] INEB - Instituto de Engenharia Biomédica
Laboratório de Sinal e Imagem; Campus FEUP (Faculdade de Engenharia da Universidade do Porto), Rua Roberto Frias, s/n, 4200-465 Porto, Portugal
[2] Universidade do Porto, Faculdade de Engenharia, DEEC
{cmsp,amendon,campilho}@fe.up.pt

Abstract. This paper presents an automated method for the selection of a set of lung nodule candidates, which is the first stage of a computer-aided diagnosis system for the detection of pulmonary nodules. An innovative operator, called sliding band filter (SBF), is used for enhancing the lung field areas. In order to reduce the influence of the blood vessels near the mediastinum, this filtered image is multiplied by a mask that assigns to each lung field point an *a priori* probability of belonging to a nodule. The result is further processed with a watershed segmentation method that divides each lung field into a set of non-overlapping areas. Suspicious nodule locations are associated with the regions containing the highest regional maximum values. The proposed method, whose result is an ordered set of lung nodule candidate regions, was evaluated on the 247 images of the JSRT database with very promising results.

1 Introduction

The detection of pulmonary nodules in chest radiography is one of most studied problems in X-ray image analysis, and many computerized schemes have been developed aiming at obtaining a solution for this important problem. Most of the proposed computer-aided diagnosis (CAD) systems adopt a two-stage approach, with an initial selection of nodule candidates, followed by the reduction of false positives, frequently based on the extraction of features and classification of the pre-selected areas.

In the system proposed by Wei *et al.* [1], the location of tumor candidates is performed by an adaptive ring filter, and afterwards 210 features are evaluated to look for the optimum feature set for discriminating between normal and abnormal regions. Keserci *et al.* [2] describes an approach for the detection of lung nodules based on a combination of morphological features with an edge-guided wavelet snake model. With this combination, the authors are able to largely reduce the number of false positives. Yoshida [3] complemented this system with a method for the reduction of false positives exploring the symmetry between the two lungs and assuming that a nodule candidate region in one lung would correspond to a normal region in the other. In [4], Suzuki *et al.* reported a reduction of

J. Martí et al. (Eds.): IbPRIA 2007, Part II, LNCS 4478, pp. 170–177, 2007.

false-positives, by using the so-called multiple massive-training neural network; in this system, the scheme for obtaining the initial set of candidates is based on a difference-image technique and linear-discriminant analysis. The computer algorithm presented by Schilham *et al.* in [5] uses multi-scale approaches for both nodule candidate selection and classification; candidates are found by looking for intensity maxima in Gaussian scale space and some features for classification are taken from a multi-scale Gaussian filterbank. In a recent work [6], the same authors proposed two optional extensions to this scheme, namely candidate selection and candidate segmentation.

This paper presents an automated method for the selection of a set of lung nodule candidates, which can constitute the first stage of a CAD system for the detection of pulmonary nodules. The two lung field areas are initially enhanced with an innovative operator, the sliding band filter (SBF), which belongs to the class of convergence index (CI) filters [7]. The result is further processed with a watershed segmentation method that divides each lung field into a set of non-overlapping areas. Suspicious nodules locations are associated with the regions containing the highest regional maximum values. In order to reduce the influence of the blood vessels near the mediastinum, the filtered image is multiplied by a mask that assigns to each lung field point an *a priori* probability of belonging to a nodule. The proposed method, whose result is an ordered set of lung nodule candidate regions, is just the initial phase of a complete computer-aided diagnosis system for the detection of lung nodules in chest radiographs.

The structure of the paper is as follows. The next section gives a brief description of the new convergence index filter. Section 3 describes the candidate region selection procedure, including the implementation of the probability mask and the morphological segmentation process. The results obtained with our method for the JSRT database [8] are shown in section 4, and section 5 contains some conclusions and guidelines for future work.

2 Sliding Band Filter

The contrast in chest radiograph images is usually low and the noisy environment is frequently high, primarily due to the limitations placed on X-ray dose. These characteristics are naturally intrinsic to all the structures that can be found in these images, and in particular to lung nodules, which normally appear as local low-density rounded areas exhibiting very weak contrast against their background. As the lack of contrast was found to be a serious drawback for the effective use of image detection methods based on the magnitude of spatial differences, Kobatake and Murakami [9] proposed an adaptive filter to detect rounded convex regions, the iris filter, which evaluates the degree of convergence of gradient vectors in the neighbourhood of the pixel of interest. This concept was further extended to generate a class of new filters, the convergence index filters [7,10,11], mainly differing on the region of support used for calculating the convergence degree of the gradient vectors.

2.1 Convergence Index Filters

The convergence index filter is based on the concept of convergence degree of a gradient vector, which is calculated from the angle $\theta_i(k,l)$ of the orientation of the gradient vector at point (k,l) with respect to a reference line with direction i. If we consider a pixel of interest P with spatial coordinates (x,y), the convergence index calculated in the neighbourhood of P that is the region of support of the filter, denoted by R, is defined as the average of the convergence indices at all M points in R, as in equation (1)

$$C(x,y) = \frac{1}{M} \sum_{(k,l)\in R} \cos\theta_i(k,l) \; . \tag{1}$$

In [10], a set of filters belonging to the convergence index class was proposed for detecting lung nodules candidates on chest X-ray images. In this work, the region used for evaluating the convergence degree consists of N half-lines radiating from the pixel of interest, which are defined over a circular convex region that was established based on the expected rounded shape of the lung nodules. When different criteria are established for selecting the points on the i^{th} half-line that are used for calculating the convergence index for direction i, distinct types of filters can be obtained. The coin filter (CF) has a fixed region of support formed by all the points in the complete set of half-lines, while the iris filter (IF) is an adaptive coin filter whose region of support can change in each direction. The adaptive ring filter (ARF) uses a ring-shaped region whose radius changes adaptively.

The iris filter automatically adjusts the length of each radial line used for measuring the averaged convergence index for direction i along the n pixels ($R_{min} \leq n \leq R_{max}$) away from $P(x,y)$, as defined by equation (2), aiming at the maximization of this value. The output of the iris filter, $IF(x,y)$, is the average of the maximal convergence indices for the N half radial directions. A slightly different implementation of the iris filter is presented in [2], where the parameter R_{min} also establishes the inner limit of the filter support region.

$$IF(x,y) = \frac{1}{N} \sum_{i=0}^{N-1} \left(\max_{R_{min}\leq n\leq R_{max}} \left(\frac{1}{n} \sum_{m=1}^{n} \cos\theta_{i,m} \right) \right) \tag{2}$$

2.2 Sliding Band Filter

The new enhancement filter proposed in this paper, called sliding band filter (SBF), is also a member of the CI filter class as its output is also a measure of the degree of convergence of gradient vectors. The main difference between this new filter and the iris filter is that the SBF searches in each radial direction the band of fixed width that corresponds to the maximum degree of convergence, while in the IF the radial line always begins in the point of interest P and the number of pixels can vary from a minimum to a maximal value. As in the ARF, the width of the band used for calculating the convergence index is equal in

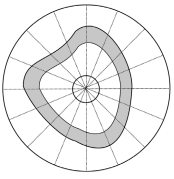

Fig. 1. Region of support of the sliding band filter

each half-line, but its position is variable in the SBF. An example of a region of support for the proposed filter is represented in Fig. 1.

The output of the SBF at a pixel of interest P is defined by equation (3),

$$SBF(x,y) = \frac{1}{N}\sum_{i=0}^{N-1}\left(\max_{R_{min}\leq n\leq R_{max}}\left(\frac{1}{d}\sum_{m=n}^{n+d}\cos\theta_{i,m}\right)\right) \tag{3}$$

where N is the number of radial directions leading out from P, d represents the fixed width of the band, $\theta_{i,m}$ is the angle of the gradient vector at the point m pixels away from P with direction i, and R_{min} and R_{max} represent, respectively, the inner and outer sliding limits of the band, as illustrated in Fig. 1.

When compared with the IF, this new approach has a more selective response for those nodules whose central region has a more random degree of convergence, because only the band of the nodule with the highest convergence indices is considered. Our proposal also has the advantage of being more flexible than the ARF when the shape of nodule differs from the expected rounded area. An original image of one lung field and enhanced images obtained with the IF, ARF and SBF are shown in Fig. 2.

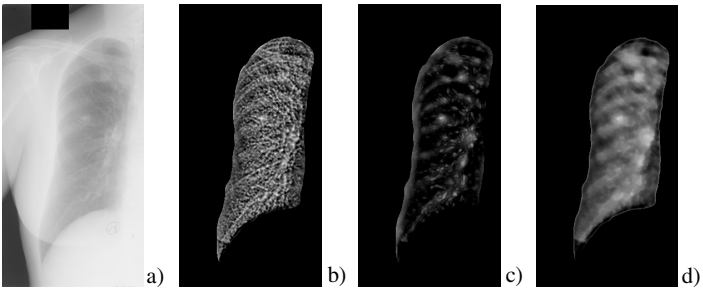

Fig. 2. a) Original lung field image; Enhanced images using: b) *IF*; c) *ARF*; d) *SBF*

3 Detection of Lung Nodule Candidate Regions

Our approach for detecting suspicious nodular regions consists of two main phases. The first phase aims at delineating and enhancing the lung field regions

using the SBF described in the previous section. In the second stage, a probability value is assigned to each lung field pixel, and afterwards these two areas are subdivided into smaller non-overlapping regions, with the goal of identifying probable locations of nodules.

3.1 Estimation of the Lung Field Probability Mask

The enhanced image resulting from the sliding band filter is strongly influenced by the blood vessels and bronchi that are located near the mediastinum. The analysis of the distribution of the nodules in the images of the JSRT database, represented in the histogram of Fig. 3a, also supports the idea that some lung field locations can have a higher probability of allocating nodules. Based on this assumption, a probability value is assigned to each lung field pixel according to equation (4),

$$P(x) = 1 - e^{-ax^n}(1 - p_0). \tag{4}$$

where x is the normalized distance of the pixel to the line parallel to the orientation axis of the lung field mask that limits the lung on the mediastinum side. In this equation a, n and p_0 are parameters, whose values of $a = 10$, $n = 4$ and $p_0 = 0.68$ were estimated from a set of randomly selected images of the JSRT database, and validated on the remaining images. These parameter values were chosen with the goal of minimizing the number of non detected nodules. The pixel distances are normalized by the width of the lung field, which is calculated as the distance between the two lines parallel to the lung field mask orientation axis, as depicted in Fig. 3b. The probability mask calculated for this particular lung field is shown in Fig. 3c.

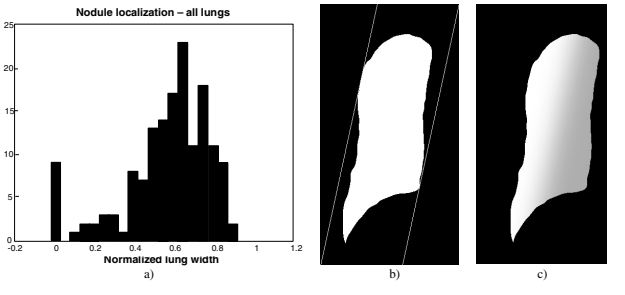

Fig. 3. a) Histogram of the nodules localization normalized by the lungs width (null distances correspond to nodules that are outside the lung field masks); b) Lung field mask with limiting lines parallel to the orientation axis; c) Probability mask

3.2 Detection of Suspicious Nodular Regions

The original radiographic image is automatically delineated aiming at obtaining two binary masks for limiting the lung field regions. Afterwards, the sliding band filter is applied thus producing enhanced images similar to the one presented

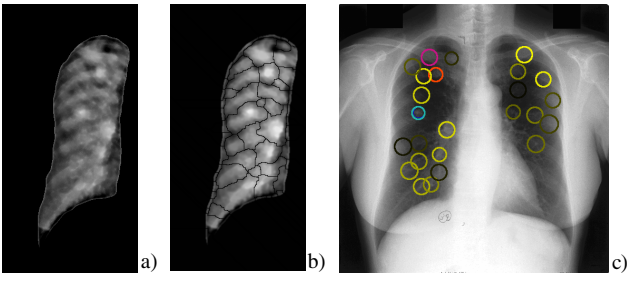

Fig. 4. a) Output of the SBF; b) Watershed segmentation result; c) Output of the algorithm showing the set of selected candidate nodules

in Fig. 2d. Each of these images is further multiplied by the corresponding probability mask described in the previous subsection.

In this new image, suspicious nodular regions are associated with local intensity maxima. However, because the number of detected points is excessive, the image is processed with a morphological watershed segmentation operator aiming at dividing each lung field into a set of non-overlapping regions, each one considered as a potential lung nodule candidate. For each of these areas, all the local maximum values are discarded except the highest one, which is regarded as a tentative center of one potential nodule. The output of the SBF for this particular point is used for candidate nodule characterization as it can be understood as the probability of being a lung nodule, while the actual filter support region gives some indication concerning probable nodule size. The output of the filter and the result of the watershed segmentation are presented in Fig. 4a and Fig. 4b, respectively.

The output of our algorithm is an ordered set of candidate image areas, corresponding to the highest filter responses. The location of each lung nodule candidate is coded using a color circumference, where the color identifies the rank of the candidate in the ordered set, and the radius of the circumference is related with the estimated size of the candidate nodule, as shown in Fig. 4c.

4 Results

The algorithm proposed in this paper was evaluated on a publicly available database, the JSRT database [8], which is a well-known dataset that has already been used by several other researchers. This database contains a total number of 247 radiographs, 154 with nodules and 93 without nodules. In our experiences, from the total set of 154 nodules, 14 are excluded as they lie outside the lung fields. From the remaining 140 radiographs with nodules, we were not able to detect other 7 nodules, thus achieving a maximum detection rate of 86.4%. These results were obtained with the SBF parameter values $N = 256$, $d = 5$, $R_{min} = 2$ and $R_{max} = 21$, which were established empirically to maximize the nodule detection rate. The IF and ARF outputs, as well as combinations of the SBF

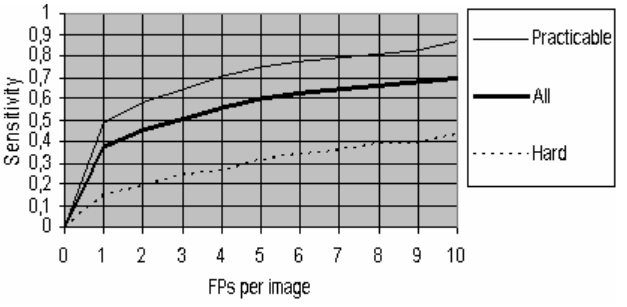

Fig. 5. FROC curves for the complete JSRT database, showing the sensitivity of our method for all nodules, for the practicable nodules (subtlety levels 3, 4 and 5 as defined in [8]) and for the hard nodules (subtlety levels 1 and 2 as defined in [8])

and ARF outputs using the arithmetic and geometric means, were also evaluated but the obtained detection rates were always lower than those achieved with the SBF alone.

In order to facilitate the comparison of our results with those recently reported by Schilham *et al.* [6], the performance of our method is presented using Free Response Receiver Operating Characteristics (FROC) curves, measuring sensitivity as a function of the average number of false positives per image, as shown in Fig. 5.

The results obtained with our algorithm are quite similar to those reported by Schilham in [6] for their basic and segmentation schemes. Despite this fact, it is worth mentioning that the values represented in Fig. 5 are essentially a consequence of the enhancement ability of the new filter in combination with the *a priori* probability assignment, which greatly facilitates the subsequent segmentation task used for detecting potential nodular areas. Actually, the output of the proposed algorithm is a just set of nodule candidate regions that are intended to be the input for a false positive reduction stage that will validate or reject each element of this set, thus reducing the number of final probable nodular regions to be presented to the specialist.

5 Conclusion

We have presented a method for the detection of suspicious regions that is just the initial phase of a more complete computer-aided diagnosis system for the detection of pulmonary nodules. The new member of the convergence index filter class proposed in this paper, the sliding band filter, has proved to be more selective than reported alternatives for the enhancement of nodular structures in pulmonary images, as the filtered image can be easily segmented to produce a reduced set of non-overlapping regions which can be associated with probable nodule candidates. The previous assignment of a probability value to each lung field pixel was also an important achievement to reduce the number of false positives associated with blood vessels and other round-shaped structures.

The algorithm was evaluated on a publicly available database, the JSRT database, which has already been used by other researchers for the assessment of lung nodules detection schemes. With an average of two false positives per image, our method achieved a sensitivity of 0.45, while this value is increased to 0.55 when four false positives are accepted. These results can be considered very promising, because we intend to use this initial set of candidates as input for a final stage of classification that will further validate or reject each one of these candidates as a probable lung nodule.

References

1. Wei, J., Hagihara, Y., Shimizu, A., Kobatake, H.: Optimal image feature set for detecting lung nodules on chest X-ray images, CARS 2002 (2002)
2. Keserci, B., Yoshida, H.: Computerized detection of pulmonary nodules in chest radiographs based on morphological features and wavelet snake model. Medical Image Analysis 6, 431–447 (2002)
3. Yoshida, H.: Local contralateral subtraction based on bilateral symmetry of lung for reduction of false positives in computerized detection of pulmonary nodules, Biomedical Engineering. IEEE Transactions 51, 778–789 (2004)
4. Suzuki, K., Shiraishi, J., Abe, H., MacMahon, H., Doi, K.: False-positive reduction in computer-aided diagnostic scheme for detecting nodules in chest radiographs by means of massive training artificial neural network. Academic Radiology 12, 191–201 (2005)
5. Schilham, A., van Ginneken, B., Loog, M.: Multi-scale Nodule Detection in Chest Radiographs. In: Ellis, R.E., Peters, T.M. (eds.) MICCAI 2003. LNCS, vol. 2878, pp. 602–609. Springer, Heidelberg (2003)
6. Schilham, A., van Ginneken, B., Loog, M.: A computer-aided diagnosis system for detection of lung nodules in chest radiographs with an evaluation on a public database. Medical Image Analysis 10, 247–258 (2006)
7. Kobatake, H., Hashimoto, S.: Convergence index filter for vector fields, IEEE Transactions on Image Processing, vol. 8(8) (1999)
8. Shiraishi, J., Katsuragawa, S., Kezoe, S., Matsumoto, T., Kobayashi, T., Komatsu, K., Matsui, M., Fujita, M., Kodera, Y., Doi, K.: Development of a Digital Image Database for Chest Radiographs With and Without a Lung Nodule: Receiver Operating Characteristic Analysis of Radiologists' Detection of Pulmonary Nodules. American Journal of Roentgenology 174, 71–74 (2000)
9. Kobatake, H., Murakami, M.: Adaptive filter to detect rounded convex regions: Iris filter. Int. Conf. Pattern Recognition ll, 340–344 (1996)
10. Wei, J., Hagihara, Y., Kobatake, H.: Detection of cancerous tumors on chest X-ray images - Candidate detection filter and its evaluation, ICIP99, no. 27AP4.2 (1999)
11. Kobatake, H., Wei, J., Yoshinaga, Y., Hagihara, Y., Shimizo, A.: Nonlinear Adaptine Convergence Index Filters and Their Characteristics, Int. Conf. Pattern Recognition, pp. 522–525 (2000)